A Note on the Shock-Capturing Properties of Some Explicit and Implicit Schemes for Solving the 1-D Linear Advection Equation.

A.R.APPADU[*]
[*] Department of Mathematics and Applied Mathematics, University of Pretoria, Pretoria 0002, South Africa. Email: Rao.Appadu@up.ac.za, biprao2@yahoo.com

Abstract
The technique of Minimized Integrated Exponential Error for Low Dispersion and Low Dissipation, **(MIEELDLD)** was introduced in Appadu and Dauhoo (2011), Appadu and Dauhoo (2009) and extensive work on this technique is reported further in Appadu (In Press), Appadu (2012). The technique enables us to assess the shock-capturing properties of numerical methods. It also allows us to find suitable values for parameters present in numerical methods in order to optimise their dissipative and dispersive properties (Appadu 2012). This technique basically makes use of a physical quantity called the Integrated Exponential Error for Low Dispersion and Low Dissipation, **IEELDLD**.
In this work, we obtain the **IEELDLD** for some explicit, quasi-implicit and implicit methods. We use **MIEELDLD** to obtain an explicit scheme with more effective shock-capturing properties than Gadd and Carpenter's numerical schemes. Also, an implicit method is constructed which is almost similar to the one derived by Dehghan (2005) and which has also better shock-capturing properties as compared to the Crank-Nicolson method.

keyword:
dispersion, dissipation, cfl number, Minimized Integrated Exponential Error for Low Dispersion and Low Dissipation.

Nomenclature:
$I = \sqrt{(-1)}$; k: time step; h: spatial step (in 1-D); β: advection velocity; r: $cfl/Courant$ number; $r = \dfrac{\beta k}{h}$; θ: wave number (in 1-D); w: phase angle in 1-D; $w = \theta h$; n: time level; RPE: relative phase error per unit time step; AF: amplification factor; AFM: Modulus of Amplification Factor; $AFM = |AF|$; **IEELDLD**: Integrated Exponential Error for Low Dispersion and Low Dissipation; **MIEELDLD**: Minimised Integrated Exponential Error for Low Dispersion and Low Dissipation.

1 Introduction

Finite difference methods (Anderson et al. 1984) are probably the most popular and often the most simple numerical approach to solve partial differential equations. They have been applied to most computational fields of science and engineering such as fluid dynamics, physical oceanography, mathematical biology, computational aeroacoustics and electromagnetics. Despite their simplicity and popularity, the design of both accurate and efficient difference methods is nontrivial.
The pioneering work of the theoretical study of finite difference scheme was made by Courant et al. (1928). Kreiss (1968) proposed the dissipation and dispersion of finite difference schemes with Fourier method. Von Neumann and Richtmyer (1950) developed Fourier analysis method of finite difference scheme. Hirt (1968) introduced the remainder analysis approach of finite difference scheme and introduced the idea of modified partial differential equation of finite difference scheme. Liu (1995) proposed the remainder-effect analysis method which combines the study of the accuracy, consistency, stability, dissipation, dispersion and group velocity effect of finite difference schemes. The remainder-effect analysis

method has been used to reform unstable schemes, control numerical dissipation, dispersion and group velocity effect in order to design and optimise finite difference schemes. Unstable schemes cannot be regarded as uninteresting as they can be reformed into stable ones. Many unstable difference schemes like Richardson scheme of the model parabolic equation can be changed under the remainder effect analysis method. Also, Wang (2010) has devised a designing algorithm which enables the construction of accurate and efficient difference methods for the 1-D linear advection-diffusion equation. His idea is based on the modified equation devised by Warming and Beam (1976).

In Computational Fluid Dynamics, shock-capturing methods are a class of techniques for computing inviscid flows with shock waves. Computation of flow through shock-waves is an extremely difficult task because such flows result in sharp, discontinuous changes in flow variables namely pressure, temperature, density, and velocity across the shock.
From an historical point of view, shock-capturing methods can be classified into two general categories namely classical methods and modern shock capturing methods (high-resolution schemes). Some examples of classical shock-capturing methods are Lax-Wendroff, Beam-Warming, Lax-Friedrichs and Fromm's schemes. Modern shock-capturing schemes include high order Total Variation Diminishing (TVD) scheme first proposed by Harten et al. (1987), Flux-Corrected Transport scheme introduced by Boris and Book (1976) and Essentially Non-Oscillatory Schemes (ENO) proposed by Harten et al. (1987).

This paper is devoted to the study of some classical numerical schemes to the 1-D linear advection equation,

$$u_t + \beta u_x = 0. \tag{1}$$

The paper is organised as follows. In section 2, we explain briefly the terms associated with the dissipation/dispersion of numerical methods. In section 3, we describe briefly our technique of optimisation namely, the Minimised Integrated Exponential Error for Low Dispersion and Low Dissipation **MIEELDLD** used to minimise dispersion/dissipation in regions of shocks. In section 4, we consider the weighted explicit finite difference formula. Based on the quantity, **IEELDLD**, we deduce that explicit methods such as Third-order Upwind, Rusanov's third order, Rusanov's fourth order and Carpenter's method are quite good shock-capturing methods. However, the Gadd (Gadd 1978) and Crowley methods (Crowley 1968) can be improved. In section 5, we propose a new explicit method baptised as AR scheme with improved shock-capturing scheme as compared to the Carpenter and Gadd schemes. In section 6, we study the shock-capturing properties of quasi-implicit schemes such as Box, Roberts and Weiss schemes. Some implicit methods are discussed in section 7. We then optimise the second order implicit scheme in section 8. In section 10, we are able to optimise a general implicit scheme which is termed as the Implicit AR scheme and show that this method is almost equivalent to the scheme proposed by Dehghan (2005) which is discussed in section 9. Lastly, concluding remarks about the salient features of this paper are included in section 11.

2 Damping and Oscillatory characteristics of numerical schemes approximating the 1-D Linear Advection Equation

All linear numerical schemes are either dispersive or dissipative (Trac and Pen 2003). In the case of dispersive schemes, oscillations are generated in regions of discontinuity. The relative phase error (RPE) is a measure of the dispersive character of a scheme. This quantity is a ratio and measures the velocity of the computed waves to that of the physical waves. It is calculated as $RPE = -\dfrac{arg(\xi)}{rw}$ (Morton and Mayers 1994), where $arg(\xi)$ denotes the argument of the amplification factor, r is the cfl number and w is the phase angle of the numerical scheme under consideration. If the RPE is greater than one, the computed waves appear to move faster than the physical waves thus causing phase lead, hence post-shock oscillations (Hirsch 1988) in regions of discontinuity. A ratio less than one implies that computed waves will move slower than physical waves, causing phase lag hence pre-shock oscillations in regions of discontinuity. A ratio of one indicates that the finite difference solution has no phase error and therefore non-physical oscillations are not present.

Dissipation is defined as the constant decrease with time of the amplitude of plane waves as they propagate in time. This causes damping behaviour to be induced especially in regions of discontinuity. If the modulus of the amplification factor is equal to one, a disturbance neither grows nor damps (Hirsch 1988). This is an ideal property for an approximation of pure convection. The modulus of the amplification factor is also a measure of the stability of a scheme. If this value is greater than one, this creates instability while damping is present whenever the value is less than one (Hirsch 1988). When the modulus of the amplification factor exceeds one, this indicates an unstable mode. The modulus of the amplification factor is denoted by AFM and is calculated as $AFM = |\xi|$, where ξ is the Amplification Factor.

3 Technique of Minimized Integrated Exponential Error for Low Dispersion and Low Dissipation

In this section, we describe briefly the technique of Minimized Integrated Exponential Error for Low Dispersion and Low Dissipation **(MIEELDLD)**. This is described in great details in Appadu and Dauhoo (2011) and further work is listed in Appadu (In press), Appadu (2012), Appadu and Dauhoo (2009).

The Von Neumann method is used to obtain the amplification factor of the numerical scheme approximating the linear advection equation. This method is based on the Fourier transform. We shall consider a single harmonic of the form $u_i^n = \xi^n \, e^{I\theta i h}$ with ξ^n being the amplification factor, θh is the phase angle and $I = \sqrt{-1}$. The amplification factor is obtained as $\xi = \dfrac{\xi^{n+1}}{\xi^n}$.

A difference scheme is considered stable for a chosen value of the Courant number, r if the modulus of the amplification factor, ξ is less than or equal to unity, for all phase angle, $w \in (0, \pi)$, over one complete time-step.

The Integrated Exponential Error for Low Dispersion and Low Dissipation, **IEELDLD** (in its simplest form) when used to find the optimal cfl of a numerical scheme is described as:

$$\textbf{IEELDLD} = \int_0^{w_1} \textbf{eeldld} \; dw,$$

where

$$\textbf{eeldld} = \exp\left(\Big||1 - RPE| - (1 - AFM)\Big|\right) + \exp(|1 - RPE| + (1 - AFM)) - 2.0, \quad (2)$$

and w_1 is a constant.

For a stable numerical scheme, the dispersion and dissipation errors are calculated as $|1 - RPE|$ and $(1 - AFM)$ respectively.

We now explain briefly how we have devised the concept of **MIEELDLD** as a technique

to control dissipation and dispersion in numerical schemes.
For a scheme to have Low Dispersion and Low Dissipation, we require

$$|1 - RPE| + (1 - AFM) \longrightarrow 0.$$

Also when dissipation neutralises dispersion optimally, we have,

$$\Big||1 - RPE| - (1 - AFM)\Big| \rightarrow 0.$$

Thus on combining these two conditions, we get the following condition necessary for dissipation to neutralise dispersion and for Low Dispersion and Low Dissipation character to be satisfied:

$$\Big||1 - RPE| - (1 - AFM)\Big| + (|1 - RPE| + (1 - AFM)) \longrightarrow 0.$$

Similarly, we expect

$$\mathbf{eeldld} = \exp\left(\Big||1 - RPE| - (1 - AFM)\Big|\right) + \exp(|1 - RPE| + (1 - AFM)) - 2 \longrightarrow 0,$$

in order for Low Dispersion and Low Dissipation properties to be achieved.
We next explain how the integration process is performed in order to obtain the optimal parameter.

Only one parameter involved

If the cfl number is the only parameter, we compute

$$\int_0^{w_1} \mathbf{eeldld}\ dw,$$

for a range of $w \in [0, w_1]$, and this integral will be a function of r. The optimal cfl is the one at which the integral quantity is closest to zero.

Two parameters are involved

We next consider a case where two parameters are involved and whereby we would like to optimise these two parameters.

Suppose we want to obtain an improved version of the Fromm's scheme which is made up of a linear combination of Lax-Wendroff (LW) and Beam-Warming (BW) schemes. Suppose we apply BW and LW in the ratio $\lambda : 1 - \lambda$. This can be done in two ways.

In the first case, if we wish to obtain the optimal value of λ at any cfl, then we compute the double integral,

$$\int_0^{r_1}\int_0^{w_1} \mathbf{eeldld}\ dw\ dr, \qquad (3)$$

which will be in terms of λ.

The value of r_1 is chosen to suit the region of stability of the numerical scheme under consideration while w_1 is chosen such that the approximated $RPE \geq 0$ for $r \in [0, r_1]$. In cases where phase wrapping phenomenon does not occur, we use the exact RPE instead of the approximated RPE and in that case, $w \in [0, \pi]$.

The second way to optimise a scheme made up of a linear combination of Beam-Warming and Lax-Wendroff is to compute the **IEELDLD** as $\int_0^{w_1}$ **eeldld** dw and the integral obtained in that case will be a function of r and λ. Then, a 3-D plot of this integral with respect to $r \in [0, r_1]$ and $\lambda \in [0, 1]$ enables the respective optimal values of r and λ to be located. The optimised scheme obtained will be defined in terms of both a cfl number and the optimal value of λ to be used.

In Appadu and Dauhoo (2011), we have obtained the optimal cfl for some explicit methods like Lax-Wendroff, Beam-Warming, Crowley, Upwind Leap-Frog and Fromm's schemes. In Appadu and Dauhoo (2009), we have combined some spatial derivatives with an optimised time derivative proposed by Tam and Webb (1993) in order to approximate the 1-D linear advection equation. The results from some numerical experiments were quantified into dispersion and dissipation errors and we have found that the quality of the results is dependent on the choice of the cfl number, even for optimised methods. In Appadu (2012), we use the technique to understand why not all composite methods can be effective to control dissipation and dispersion in regions of shocks. In Appadu (In press), we consider the family of third order methods proposed by Takacs where we optimize two parameters, namely the cfl number and another variable which also controls dispersion and dissipation. Also, the optimal cfl for some multi-level schemes has been obtained.
In this work, our aim is to compare shock-capturing properties of some numerical schemes. The phenomenon of phase wrapping can occur and hence we have to work with the approximated RPE when computing the **IEELDLD**. Since, at times we have to limit the range of w to be less than π so that the approximated $RPE \geq 0$, therefore, in this work we limit $w \in [0, 1.0]$ when computing the **IEELDLD** as this range of w will allow the approximated RPE to be calculated such that it is always greater or equal to zero.

4 Two-Level Explicit Schemes

We consider the weighted explicit finite-difference formula approximating Eq. (1) as described by Dehghan (2005):

$$\begin{aligned} u_i^{n+1} &= -\frac{r}{12}\,(6\phi+\gamma_1)\,u_{i-2}^n + \frac{r}{6}(3+3\theta+9\phi+\gamma_1)\,u_{i-1}^n \\ &-\frac{r}{6}\,(3-3\theta-3\phi+\gamma_1)\,u_{i+1}^n + \frac{r\gamma_1}{12}\,u_{i+2}^n + \frac{1}{2}\,(2-3r\phi-2r\theta)\,u_i^n, \end{aligned} \tag{4}$$

where $r = \dfrac{\beta k}{h}$.

4.1 $\theta = 1$ *and* $\gamma_1 = 0$

For the case, $\theta = 1$ and $\gamma_1 = 0$ in Eq. (4), the only method treated in Dehghan (2005) corresponds to $\phi = 0$ and the method is the Upwind scheme. The scheme is stable for $0 < r \leq 1$. Our aim here is to fix the value of θ as one and γ_1 as zero and use the technique of **MIEELDLD** to find the optimal value of ϕ.
The amplification factor for the method described by Eq.(4) for the case $\theta = 1$ and $\gamma_1 = 0$ is given by

$$\begin{aligned} \xi = 1 + (\cos(w)-1)\,r + (-1+2\,\cos(w)-\cos^2 w)\,r\phi \,+ \\ I\,r\sin(w)\Big(\phi(\cos(w)-1)-1\Big). \end{aligned} \tag{5}$$

We then compute the **IEELDLD** as

$$\int_0^1 \textbf{eeldld}\; dw.$$

The approximated RPE is given by

$$1+\frac{1}{6}\,(-1+3\phi+3r-2r^2)\;w^2+$$
$$\Big(\frac{1}{120}-\frac{1}{8}\,\phi+\Big(\frac{1}{2}\phi-\frac{1}{8}\Big)\;r+\Big(-\frac{1}{2}\phi+\frac{5}{12}\Big)\;r^2-\frac{1}{2}\;r^3+\frac{1}{5}\;r^4\Big)\;w^4. \tag{6}$$

We obtain the contour plot of the **IEELDLD** vs ϕ vs r in Fig. (1(a)) and it is seen that the **IEELDLD** values are closest to zero for $\phi = 0$ and $r = 1$. We also examine whether there exists a relationship between ϕ and r which corresponds to an optimised method. Thus, we obtain a contour plot of the **IEELDLD** vs ϕ vs r for the least possible values of **IEELDLD**, in that case, **IEELDLD** $\in [1\times 10^{-4}, 1\times 10^{-3}]$. The plot is shown in Fig. (1(b)) and we see that a possible relationship can be $\phi = 1 - r$.
Thus, we can conclude the following. If we fix $\theta = 1$ and $\gamma_1 = 0$, we get an optimised method when $r \longrightarrow 1$ and $\phi \longrightarrow 0$. Also, for $r \longrightarrow 1$ and $\phi \longrightarrow 0$, we observe that the optimal relation can be described by $\phi = 1 - r$.

4.2 $\theta = r$ *and* $\gamma_1 = 0$

For the case $\theta = r$ and $\gamma_1 = 0$, four explicit methods have been described in Dehghan (2005). These are:
(a) Leith or Lax-Wendroff (Lax and Wendroff 1960) with $\phi = 0$ and the range of stability is $0 < r \leq 1$.
(b) Beam-Warming (Warming and Beam 1976) with $\phi = 1 - r$ and $r \in [0, 2]$.
(c) Fromm (Fromm 1968) with $\phi = \dfrac{1-r}{2}$ and $r \in [0, 1]$.
(d) Third order Upwind (Leonard 1984) scheme with $\phi = \dfrac{1-r^2}{3}$ and $r \in [0, 1]$.

In this section, we fix $\theta = r$ and $\gamma_1 = 0$ in Eq. (4) and find out whether any of the numerical schemes described above in (a), (b), (c), (d) can be recovered when we use **MIEELDLD**. The amplification factor of the method described in Eq. (4) for the case $\theta = r$ and $\gamma_1 = 0$ is given by

$$\begin{aligned}\xi &= 1+(-\cos^2 w+2\cos w-1)\;r\phi+(\cos(w)-1)r^2\\ &\quad +I\;r\;\sin(w)\;\Big((\cos(w)-1)\phi-1\Big).\end{aligned} \tag{7}$$

The approximated RPE is

$$1+\frac{1}{6}\,(3\phi-1+r^2)\;w^2+\frac{1}{120}\,(1-15\;\phi+30\;\phi\;r+5r^2-6r^4)\;w^4. \tag{8}$$

We next compute the **IEELDLD** which is a function of r and ϕ. We obtain contour plot of the **IEELDLD** vs r vs ϕ in Fig. (2(a)). Zoomed plot for the least possible values of **IEELDLD**, in that case, **IEELDLD** $\in [1\times 10^{-4}, 5\times 10^{-4}]$ is shown in Fig. (2(b)).
We also observe that a linear relationship between ϕ and r exists which gives rise to an optimised scheme for $r \to 1$ and $\phi \to 0$ as shown in Fig. 2(b). This relationship is $\phi = \dfrac{1-r}{2}$ which actually corresponds to the Fromm's scheme.

To summarise, four methods are possible for $\theta = r$ and $\gamma_1 = 0$. By fixing $\theta = r$ and $\gamma_1 = 0$ in Eq.(4) and applying **MIEELDLD**, we observe that an optimised scheme is possible and it corresponds to the Fromm's method for the special case: $\phi \to 0$ and $r \to 1$.

4.3 Third order Upwind

The third-order upwind scheme (Leonard 1984) is described by Eq. (4) for the case $\theta = r$, $\phi = \dfrac{1-r^2}{3}$ and $\gamma_1 = 0$. It has been described as being a very robust and efficient algorithm for computational fluid mechanics.
On replacing θ by r and ϕ by $\left(\dfrac{1-r^2}{3}\right)$, the amplification factor of the resulting method is given by

$$\begin{aligned}\xi = 1 + \frac{r}{3}\,(-\cos^2 w + 2\cos(w) - 1) + r^2\,(\cos(w) - 1) + \\ \frac{r^3}{3}\,(\cos^2 w - 2\cos(w) + 1) + I\,\frac{r\sin(w)}{3} \\ \Big((\cos(w) - 4 + \gamma_1(\cos(w) - 1) + r^2\sin(w)(1 - \cos(w))\Big).\end{aligned} \tag{9}$$

A contour plot of the **IEELDLD** vs γ_1 vs r is illustrated in Fig. (3(a)) and we observe that the values are least as $\gamma_1 \longrightarrow 0$. By limiting the range of **IEELDLD** $\in (1\times10^{-3}, 9\times10^{-3})$, we observe that the **IEELDLD** is least especially for $\gamma_1 \longrightarrow 0$ and $r \longrightarrow 1$, as depicted in Fig. (3(b)). However, it is quite difficult to find a relationship for γ_1 as a function of r which defines the least possible values of **IEELDLD**.

4.4 Rusanov's third order scheme

On plugging $\theta = r$, $\phi = \dfrac{2(1-r^4)}{15\,r}$ and $\gamma_1 = \dfrac{(r^2-1)\,(1-2r)\,(2-r)}{5\,r}$ in Eq. (4), we obtain the Rusanov's third order method (Rusanov 1970).
We fix $\theta = r$ and $\phi = \dfrac{2\,(1-r^4)}{15r}$ in Eq. (4) and use **MIEELDLD** to study the dependency of γ_1 on r which optimises the shock-capturing property of the method.
The amplification factor for the method described by Eq. (4) for the case $\theta = r$ and $\phi = \dfrac{2(1-r^4)}{15r}$, is given by

$$\begin{aligned}\xi = \frac{1}{15}\,(13 + 4\,\cos(w) - 2\cos^2 w) + (\cos(w) - 1)\,r^2 + \\ \frac{2}{15}r^4(1 - 2\cos(w) + \cos^2 w) + \\ I\,\Big(\Big(\frac{\gamma_1\sin(w)}{3}(\cos(w) - 1) - \sin(w)\Big)r + \frac{2}{15}\,r^2\,\sin(w)(\cos(w) - 1) + \\ \frac{2}{15}r^4\sin(w)(1 - \cos(w))\Big).\end{aligned} \tag{10}$$

The approximated RPE is

$$\begin{aligned}1 + \frac{1}{30}\,\Big(\frac{2}{r} - 5 + 5\gamma_1 + 5r^2 - 2r^3\Big)w^2 \\ + \frac{1}{120}\Big(-\frac{2}{r} + 5(1-\gamma_1) - 4r + 5(1-2\gamma_1)r^2 + 2r^3 - 10r^4 + 4r^5\Big)\,w^4.\end{aligned} \tag{11}$$

We plot the variation of **IEELDLD** vs γ_1 vs r in Figs. (4(a)) and (4(b)), we observe that the least values of **IEELDLD** lie
(i) close to $\gamma_1 = -3$ and $r = 0.05$.
(ii) close to $\gamma_1 = -1$ and $r = 0.2$.
(iii) close to $\gamma_1 = -0.5$ and $r = 0.3$.
(iv) close to $\gamma_1 = 0$ and $0.4 \le r \le 1$.

We now plot the variation of γ_1 vs r for the Rusanov third order scheme. Interestingly, based on Figs. (4(b)) and (9(a)), we can conclude that the variation represented by $\gamma_1 = \dfrac{(r^2-1)(1-2r)(2-r)}{5\,r}$ fits into the region for very low **IEELDLD** values. Thus, we expect the Rusanov's third method to be quite an efficient shock-capturing method.

4.5 Rusanov's fourth-order method

On plugging $\theta = r$, $\phi = \dfrac{r(1-r^2)}{6}$ and $\gamma_1 = \dfrac{(2-r)\,(1-r^2)}{2}$ in Eq. (4), we obtain the Rusanov's fourth-order method.
We replace θ by r and ϕ by $\dfrac{r(1-r^2)}{6}$ in Eq. (4). The amplification factor of the resulting method is

$$\begin{aligned}\xi = 1 + \frac{r^2}{6}\,(-\cos^2 w + 8\cos(w) - 7) + \frac{r^4}{6}\,(\cos^2 w - 2\cos(w) + 1)\\ +I\,\Big(- r\sin(w) + \frac{1}{3}\,r\gamma_1 \sin(w)(\cos(w) - 1)\\ +\frac{r^2}{6}\sin(w)(\cos(w)-1) + \frac{r^4}{6}\,\sin(w)(1-\cos(w))\Big).\end{aligned} \tag{12}$$

A contour plot of the **IEELDLD** vs γ_1 vs r is shown in Fig. (5(a)). To gain more insight, we obtain a contour plot of the least possible values of **IEELDLD** $\in [1\times10^{-3}, 1\times10^{-2}]$ in Fig. (5(b)) and we observe that the lowest values of **IEELDLD** can be obtained for curves approximating the line $\gamma_1 = 1 - r$. We plot the variation of γ_1 vs r in Fig. (9(b)). Based on Figs. (5(b)) and (9(b)), we can conclude that the variation of $\gamma_1 = \dfrac{(2-r)\,(1-r^2)}{2}$ results in a scheme with quite good shock capturing properties. Hence, we conclude that the Rusanov fourth order scheme is effective to resolve discontinuities.

4.6 Carpenter's method

The Carpenter's method (Carpenter 1979) is obtained on substituting θ by r, ϕ by $\dfrac{r(1-r^2)}{3}$ and γ_1 by $(1-r^2)\,(1-r)$ in Eq. (4).
Our aim here is to replace θ by r and ϕ by $\dfrac{r\,(1-r^2)}{3}$ in Eq. (4). We then obtain the amplification factor of the resulting scheme and use **MIEELDLD** to seek whether the relationship given by $\gamma_1 = (1-r^2)(1-r)$ optimises the shock-capturing properties of the scheme.

The amplification factor of the resulting method is

$$\xi = 1 + \frac{r^2}{3}\ (-\cos^2 w + 5\cos(w) - 4) + \frac{r^4}{3}\ (\cos^2 w - 2\ \cos(w) + 1)$$
$$+I\ \Big(-r\sin(w) + \frac{\gamma_1}{3}\ r\ \sin(w)(\cos(w)-1) + \frac{r^2}{3}\ \sin(w)(\cos(w)-1)$$
$$+\frac{r^4}{3}\sin(w)(1-\cos(w))\Big). \tag{13}$$

We then obtain the contour plot of the **IEELDLD** as a function of γ_1 and r.
The contour plot of **IEELDLD** vs γ_1 vs r is shown in Fig. (6(a)). We obtain a contour plot of the least possible values of **IEELDLD**, (in that case we have **IEELDLD** $\in [1 \times 10^{-3}, 9 \times 10^{-3}]$) in Fig. (6(b)).
We also plot also the variation of γ_1 vs r which defines the Carpenter's method in Fig. (9(c)).
There is an interesting connection between the graphs of Figs. (6(b)) and (9(c)) which indicates that the variation of γ_1 vs r which defines the Carpenter's method yields an optimised method with good shock-capturing properties.

4.7 Gadd's technique

The Gadd method (Gadd 1978) is described by Eq.(4) for the case $\theta = r$, $\phi = \dfrac{r\ (1-r^2)}{2}$ and $\gamma_1 = \dfrac{3(1-r^2)\ (1-r)}{2}$.
On replacing θ by r and ϕ by $\dfrac{r(1-r^2)}{2}$ in Eq. (4) and applying the Von Neumann Stability Analysis, we obtain the amplification factor of the resulting method as

$$\xi = 1 + (-0.5\cos^2 w + 2\cos w - 1.5)r^2 + 0.5(\cos^2 w - 2\cos(w) + 1)r^4$$
$$+I\Big(\frac{r\sin(w)}{3}(-3 - \gamma_1 + \gamma_1\cos(w)) + 0.5r^2\sin(w)(\cos(w)-1) +$$
$$0.5r^4\sin(w)(2-\cos(w))\Big). \tag{14}$$

A contour plot of **IEELDLD** vs γ_1 vs r is shown in Fig. (7(a)). A contour plot for **IEELDLD** $\in [2 \times 10^{-3}, 1.2 \times 10^{-2}]$ is shown in Fig. (7(b)). A plot of γ_1 vs r is shown in Fig. (9(d)). On comparing the plots, we observe that the variation of γ_1 vs r in Fig. (9(d)) does not correspond to very low values of **IEELDLD**. So, we conclude that the Gadd's scheme does not have very good shock-capturing properties. Hence, the variation of $\gamma_1 = \dfrac{(1-r^2)(1-r)}{2}$ vs r is not an optimal variation which optimises the shock-capturing properties of the method.

4.8 Crowley

The Crowley scheme (Crowley 1968) can be obtained from Eq. (4) on fixing $\theta = r$, $\phi = -\dfrac{r}{2}$ and $\gamma_1 = \dfrac{3r(2-r)}{4}$. On replacing θ by r and ϕ by $-\dfrac{r}{2}$ in Eq. (4) and using Von Neumann stability, we obtain the amplification factor of the resulting method as:

$$\xi = 1 - 0.5\ r^2(1-\cos^2 w)$$
$$+I\ \Big(\frac{r}{3}\ \sin(w)(-3 + \gamma_1\cos(w) - \gamma_1) + 0.5\ r^2\sin(w)(1-\cos(w))\Big). \tag{15}$$

The approximated RPE is given by

$$1+\frac{1}{12}(-2+2\gamma_1-3r+2r^2)\ w^2+ \left(\frac{1}{120}-\frac{\gamma_1}{24}+\frac{1}{16}r-\frac{1}{12}\ (1+\gamma_1)\ r^2+\frac{1}{8}\ r^3-\frac{1}{20}\ r^4\right)\ w^4. \tag{16}$$

A contour plot of **IEELDLD** vs γ_1 vs r is shown in Fig. (8(a)). To get more information on the contour plot, we obtain a contour plot with the least possible values of **IEELDLD**, in that case we have, **IEELDLD** $\in [0.04, 0.065]$ and the plot is shown in (8(b)). The variation of γ_1 vs r which defines the Crowley method is shown in Fig. (9(e)) and we can observe that it is not one which optimises the shock-capturing property of the Crowley scheme. Hence, the existing Crowley method can be improved to generate an improved method in terms of shock-capturing properties.

5 Explicit AR scheme

We can see that there is a connection between the Carpenter's scheme and the Gadd scheme. They can both be obtained from Eq. (4) on replacing θ by r and ϕ and γ_1 as functions of r.
In the case of Carpenter's method we have $\gamma_1 = (1-r^2)\ (1-r)$ and $\phi = \dfrac{r(1-r^2)}{3}$ while in the case of Gadd, we have $\gamma_1 = \dfrac{3\ (1-r^2)(1-r)}{2}$ and $\phi = \dfrac{r(1-r^2)}{2}$. From the work in sections 4.6 and 4.7, we have deduced that the Gadd's method can be improved.
So, we try to obtain an improvement over these two methods. We consider Eq. (4) and replace θ by r, ϕ by $ar(1-r^2)$ and $\gamma_1 = b(1-r^2)\ (1-r)$ where a and b are parameters to be determined using **MIEELDLD**.
We note that for $a = \dfrac{1}{3}$, $b = 1$ we recover Carpenter's method and for $a = \dfrac{1}{2}$ and $b = \dfrac{3}{2}$, the Gadd's scheme is obtained.
We compute the **IEELDLD** for the numerical method described by Eq. (4) with $\theta = r$, $\phi = ar(1-r^2)$ and $\gamma_1 = b(1-r^2)(1-r)$. The **IEELDLD** is computed as

$$\int_0^1 \int_0^1 \mathbf{eeldld}\ dw\ dr. \tag{17}$$

A contour plot of the **IEELDLD** with respect to a and b is shown in Fig. (10(a)). The contour plot in Fig. (10(b)) shows contour lines for very low values of **IEELDLD** $\in [6\times10^{-3}, 7\times10^{-3}]$.

We observe that the optimal values of a and b are approximately 0.4 and 1.0 respectively. We baptise the optimised method as the explicit AR scheme.
We now compare the variation of the **IEELDLD** vs r for the Carpenter's method, the Gadd's scheme and the explicit AR scheme, for phase angles, $w \in [0, 1.0]$ in Fig. (11). We observe that the Explicit AR scheme is slightly better than Carpenter's method. Also, the Explicit AR method is much better than the Gadd's scheme. We compare the dissipative and dispersive properties of the Explicit AR scheme and the Carpenter's scheme at some different cfl numbers. We choose $w \in [0, \pi]$ to have a better idea of the shock-capturing property of the methods over a wider range of phase angles. Since the RPE is a function of only the phase angle when the cfl number is fixed, the phase wrapping phenomenon can be alleviated when using the exact RPE. The plots are shown in Figs. (12(a)) and (12(b)). It

is observed that the AR scheme and Carpenter's scheme have almost the same variation for the plot of the AFM vs phase angle, at the cfl numbers 0.25 and 0.50. However, the AR scheme is less dissipative than Carpenter's method at cfl 0.75. The variation of the RPE vs phase angle is shown in Fig. (12(b)). We observe that the AR scheme is slightly less dispersive at cfl 0.25 and also less dispersive at cfl 0.50, as compared to the Carpenter's method. However, the AR scheme is slightly more dispersive as compared to Carpenter's method at cfl 0.75. Based on Fig. (11), we can conclude that the AR Explicit method is in general slightly better than the Carpenter's method.

6 Quasi-implicit methods

We consider two quasi-implicit schemes namely the box scheme and the Roberts and Weiss scheme (Roberts and Weiss 1966). Our aim is to check how efficient these methods are in terms of shock-capturing properties on plotting the variation of **IEELDLD** vs cfl number for both methods, as shown in Fig. (13).

6.1 Box method

The amplification factor is

$$\xi = \frac{\Big((1-r)+(1+r)\ \cos(w)\Big) - I\ (1+r)\ \sin(w)}{\Big((1+r)+(1-r)\ \cos(w)\Big) - I\ (1-r)\ \sin(w)}. \tag{18}$$

The method is regarded as quasi-implicit. This is because, though the method is implicit, the values of u_i^{n+1} can be computed in an explicit manner using the formula:

$$u_i^{n+1} = u_{i-1}^n + \Big(\frac{1-r}{1+r}\Big)(u_i^n - u_{i-1}^{n+1}). \tag{19}$$

The method is unconditionally stable. Fig. (13(a)) shows that the method is most efficient at cfl 1.0. On plugging, $r = 1$ in Eq. (4), we get $u_i^{n+1} = u_{i-1}^n$. Hence, the method becomes explicit at $r = 1$ and also shift condition is satisfied at $r = 1$.

6.2 Roberts and Weiss scheme

We use $\dfrac{\partial u}{\partial t} \approx \dfrac{u_i^{n+1} - u_i^n}{2\ k}$ and $\dfrac{\partial u}{\partial x} \approx \dfrac{1}{2}\left(\dfrac{u_i^{n+1} - u_{i-1}^{n+1}}{h} + \dfrac{u_{i+1}^n - u_i^n}{h}\right)$ to obtain the Roberts and Weiss scheme as:

$$-r\ u_{i-1}^{n+1} + (2+r)\ u_i^{n+1} = (2+r)\ u_i^n - r\ u_{i+1}^n. \tag{20}$$

Its amplification factor is given by

$$\xi = \frac{A - I\ B}{A + I\ B}, \tag{21}$$

where

$$A = 1 - \frac{r}{2+r}\cos(w)$$

and

$$B = \frac{r}{2+r}\sin(w).$$

The scheme is unconditionally stable. Based on the plots in Fig. (13), we can conclude that the Box scheme has in general superior shock-capturing properties than the Roberts and Weiss scheme. Also, the Roberts and Weiss scheme is less effective at larger cfl numbers.

7 Implicit methods

We compare the shock-capturing properties of some existing implicit methods such as Backward in Time and Centred in Space Scheme (BTCS), Crank-Nicolson (Crank and Nicolson 1947) and a second-order implicit method (Dehghan 2005). We then propose some implicit methods and analyse how effective these methods are, in order to control computational noise in regions of shocks.

7.1 Backward in Time and Centred in Space Scheme

On approximating the time derivative by a backward approximation and using a centred approximation for the spatial derivative, we get the following implicit method:

$$r\ u_{i+1}^{n+1} + 2\ u_i^{n+1} - r\ u_{i-1}^{n+1} = 2\ u_i^n. \tag{22}$$

The amplification factor of the scheme is given by

$$\xi = \frac{1 - (r\sin(w))\ I}{1 + r^2\ \sin^2 w}. \tag{23}$$

The method is unconditionally stable. A plot of **IEELDLD** vs r is shown in Fig. (14). The values of **IEELDLD** are rather large and this indicates that the method is not a very effective shock-capturing method.

7.2 Crank-Nicolson method

On approximating $\dfrac{\partial u}{\partial t}$ by

$$\Big(\frac{u_i^{n+1} - u_i^n}{k}\Big) \tag{24}$$

and $\dfrac{\partial u}{\partial x}$ by

$$\Big(\frac{u_{i+1}^n - u_{i-1}^n}{2h} + \frac{u_{i+1}^{n+1} - u_{i-1}^{n+1}}{2h}\Big), \tag{25}$$

the Crank-Nicolson scheme is obtained. A single expression for the Crank Nicolson method when used to discretise the linear advection equation is

$$r\ u_{i+1}^{n+1} + 4\ u_i^{n+1} - r\ u_{i-1}^{n+1} + r\ u_{i+1}^n - r\ u_{i-1}^n - 4\ u_i^n = 0. \tag{26}$$

The amplification factor of the method is given by

$$\xi = \frac{1 - 0.5I\ r\ \sin(w)}{1 + 0.5\ I\ r\ \sin(w)}. \tag{27}$$

A plot of the RPE vs r vs w is shown in Fig. (15(a)) and we observe that for a given value of w, RPE is almost independent of the cfl number. A plot of the **IEELDLD** vs r is shown in Fig. (15(b)) and we observe that the **IEELDLD** values are very close to zero and also independent of the cfl number. Hence, the method is very efficient to control computational noise at any value of cfl. We can explain why the **IEELDLD** is independent of the cfl. This is because we have $AFM = 1$ and also the RPE is almost independent of the cfl at a given value of w, as depicted in Fig. (15(a)).

7.3 The second order implicit method

A second order implicit method is described in Dehghan (2005). The partial derivative $\frac{\partial u}{\partial t}$ is approximated by

$$\frac{1}{6}\Big(\frac{u_{i-1}^{n+1}-u_{i-1}^{n}}{k}\Big)+\frac{1}{6}\Big(\frac{u_{i+1}^{n+1}-u_{i+1}^{n}}{k}\Big)+\frac{2}{3}\Big(\frac{u_{i}^{n+1}-u_{i}^{n}}{k}\Big), \tag{28}$$

while $\frac{\partial u}{\partial x}$ is approximated by

$$\frac{1}{4}\Big(\frac{u_{i+1}^{n}-u_{i-1}^{n}}{h}\Big)+\frac{1}{4}\Big(\frac{u_{i+1}^{n+1}-u_{i-1}^{n+1}}{h}\Big). \tag{29}$$

The method is described as

$$2(u_{i-1}^{n+1}-u_{i-1}^{n}+u_{i+1}^{n+1}-u_{i+1}^{n})+8\ (u_{i}^{n+1}-u_{i}^{n})+3r(u_{i+1}^{n}-u_{i-1}^{n}+u_{i+1}^{n+1}-u_{i-1}^{n+1})=0. \tag{30}$$

A single expression for the second-order implicit scheme is given by:

$$(2-3r)\ u_{i-1}^{n+1}+(2+3r)\ u_{i+1}^{n+1}+8\ u_{i}^{n+1}=(2+3r)\ u_{i-1}^{n}+8\ u_{i}^{n}+(2-3r)\ u_{i+1}^{n}. \tag{31}$$

8 Optimising the second order implicit method

In this section, we attempt to modify the parameters in the scheme described in section 7.3 in an attempt to optimise its dispersive and dissipative properties. We approximate $\frac{\partial u}{\partial t}$ as

$$\alpha\Big(\frac{u_{i-1}^{n+1}-u_{i-1}^{n}}{k}\Big)+\alpha\Big(\frac{u_{i+1}^{n+1}-u_{i+1}^{n}}{k}\Big)+(1-2\alpha)\frac{u_{i}^{n+1}-u_{i}^{n}}{k}, \tag{32}$$

where α is a parameter to be determined.
The spatial derivative, $\frac{\partial u}{\partial x}$ is approximated by

$$\Big(\frac{u_{i+1}^{n}-u_{i-1}^{n}}{2h}\Big)+\Big(\frac{u_{i+1}^{n+1}-u_{i-1}^{n+1}}{2h}\Big). \tag{33}$$

On combining Eqs. (32) and (33), we obtain

$$\begin{aligned}\Big(\alpha+\frac{r}{4}\Big)u_{i+1}^{n+1}+(1-2\alpha)u_{i}^{n+1}+\Big(\alpha-\frac{r}{4}\Big)u_{i-1}^{n+1}&=\\ \Big(\alpha-\frac{r}{4}\Big)u_{i+1}^{n}+(1-2\alpha)u_{i}^{n}+\Big(\alpha+\frac{r}{4}\Big)u_{i-1}^{n}.\end{aligned} \tag{34}$$

The amplification factor of the numerical scheme given by Eq. (34) is given by

$$\xi=\frac{2\alpha(\cos(w)-1)+1-I\ (r/2)\sin(w)}{2\alpha(\cos(w)-1)+1+I\ (r/2)\sin(w)}. \tag{35}$$

Clearly, the method is unconditionally stable. The approximated RPE is

$$1+\Big(-\frac{1}{6}+\alpha-\frac{1}{12}\,r^2\Big)\,w^2. \tag{36}$$

We compute the **IEELDLD** as

$$\int_0^1 \textbf{eeldld}\;dw.$$

Plots of the **IEELDLD** vs α vs r are shown in Figs. (16). Contour plot with the least possible values of **IEELDLD**, in that case, **IEELDLD** values $\in[2\times10^{-3},2\times10^{-2}]$ is shown in Fig. (16(b)). This study shows that the scheme given by Eq. (34) can be optimised for α close to 0.5 and r close to 2. However, it is not possible to determine an optimal value of α at a general value of cfl that enables the method to have very good shock-capturing properties.

9 Construction of an Implicit scheme by Dehghan (2005)

The linear advection equation is approximated such that

$$\frac{\partial u}{\partial t}\approx\Big(\frac{2+r^2}{12}\Big)\Big(\frac{u_{i-1}^{n+1}-u_{i-1}^{n}}{k}\Big)+\Big(\frac{4-r^2}{12}\Big)\Big(\frac{u_{i}^{n+1}-u_{i}^{n}}{k}\Big)+\Big(\frac{2+r^2}{12}\Big)\Big(\frac{u_{i+1}^{n+1}-u_{i+1}^{n}}{k}\Big) \tag{37}$$

and

$$\frac{\partial u}{\partial x}=\frac{1}{2}\,\Big(\frac{u_{i+1}^{n}-u_{i-1}^{n}}{2h}+\frac{u_{i+1}^{n+1}-u_{i-1}^{n+1}}{2h}\Big). \tag{38}$$

The implicit method developed by Dehghan (2005) to approximate Eq. (1) is given by

$$\begin{aligned}(r^2+3r+2)\;u_{i+1}^{n+1}+2(4-r^2)\;u_{i}^{n+1}+(r^2-3r+2)\;u_{i-1}^{n+1}&=\\(r^2-3r+2)\;u_{i+1}^{n}+2(4-r^2)\;u_{i}^{n}+(r^2+3r+2)\;u_{i-1}^{n}.&\end{aligned} \tag{39}$$

The amplification factor of the method is given by

$$\xi=\frac{A-I\;B}{A+I\;B}, \tag{40}$$

where
$A=4\;(2+\cos(w))+2\;r^2(\cos(w)-1)$ and $B=6r\sin(w)$.

The method is unconditionally stable. An approximation to the RPE is

$$1+\Big(-\frac{1}{180}+\frac{1}{144}r^2-\frac{1}{720}\;r^4\Big)w^4. \tag{41}$$

A plot of the **IEELDLD** vs r is shown in Fig. (18). We observe that the **IEELDLD** values $\in[0,0.023]$ for $r\in[0,2.2]$ for all phase angles $\in[0,1.0]$. We deduce that this method has better shock-capturing properties than the Crank-Nicolson method for phase angles, $w\in[0,1]$ and $r\in[0,2.2]$. We observe that the optimal cfl is 1 or 2. But, since the method is not solvable for $r>1$ as pointed out in Dehghan (2005), we conclude that the method is most effective at $cfl=1$.

10 Construction of an implicit scheme using the technique of MIEELDLD

Based on the numerical scheme proposed by Dehghan (2005) in section 9, we set the approximation for the time derivative as

$$\frac{\partial u}{\partial t} \approx (a + b\ r^2)\left(\frac{u_{i-1}^{n+1} - u_{i-1}^{n}}{k}\right) + (1 - 2\ a - 2\ b\ r^2)\left(\frac{u_{i}^{n+1} - u_{i}^{n}}{k}\right) + (a + b\ r^2)\left(\frac{u_{i+1}^{n+1} - u_{i+1}^{n}}{k}\right), \tag{42}$$

and

$$\frac{\partial u}{\partial x} = \frac{1}{2}\left(\frac{u_{i+1}^{n} - u_{i-1}^{n}}{2h} + \frac{u_{i+1}^{n+1} - u_{i-1}^{n+1}}{2h}\right).). \tag{43}$$

We note that for the case $a = \frac{2}{12}$, $b = \frac{1}{12}$, Eq.(42) corresponds to the time derivative used by Dehghan (2005).

On combining Eqs. (42) and (43), we obtain our proposed numerical scheme as

$$(a + br^2)\ (u_{i-1}^{n+1} - u_{i-1}^{n}) + (1 - 2\ a - 2\ br^2)\ (u_{i}^{n+1} - u_{i}^{n}) + (a + b\ r^2)\ (u_{i+1}^{n+1} - u_{i+1}^{n}) + \frac{r}{4}(u_{i+1}^{n} - u_{i-1}^{n}) + \frac{r}{4}(u_{i+1}^{n+1} - u_{i-1}^{n+1}) = 0. \tag{44}$$

We obtain the amplification factor as

$$\xi = \frac{A - I\ B}{A + I\ B},$$

where $A = (4a + 4\ b^2)\cos(w) + (2 - 4a - 4b\ r^2)$ and $B = r\sin(w)$.

We compute $\int_0^{2.0}\int_0^{1.0}$ **eeldld** $dwdr$. This integral will be a function of a and b. We obtain contour plots of **IEELDLD** vs b vs a in Figs. (17(a)) and (17(b)). Fig. (17(b)) shows the least possible values of **IEELDLD** $\in [0.00155, 0.004]$. The range of optimal values of a and b obtained using **MIEELDLD** include the values used by Dehghan. Clearly, the numerical scheme given by Eq. (42) with a and b equal to 0.1692 and 0.0814 respectively have smallest **IEELDLD** values approximately equal to 0.00155 whereas the smallest **IEELDLD** values for Crank-Nicolson are 0.08, for $r \leq 2.0$. The plot of the **IEELDLD** vs r for the Implicit AR scheme is almost identical to that obtained in the case of the Implicit scheme derived by Dehghan, as illustrated in Fig. (18).

11 Conclusions

This study reveals that implicit numerical methods like Crank-Nicolson and the implicit scheme constructed by Dehghan (2005) are very good numerical methods as compared to other implicit schemes like Box, Roberts and Weiss, second-order implicit methods to control numerical noise in regions of discontinuities for the 1-D linear advection equation. The choice of the cfl number affects explicit schemes and some implicit methods like Box scheme and Roberts and Weiss scheme. However, the choice of cfl number is not very important for implicit methods like Crank-Nicolson. We have optimised the parameters for a general implicit scheme and able to demonstrate that the new method termed as implicit AR method has noticeably improved dissipation/dispersion properties as compared to Crank-Nicolson method for cfl numbers less than 2.0. the Implicit AR scheme has better shock-capturing properties than the scheme devised by Dehghan for $0 < r < 1.8$. Moreover, we have been able to obtain an improved explicit method over the Gadd and Carpenter numerical schemes. In a nutshell, we conclude that the technique of Minimised Integrated Exponential Error, **MIEELDLD** enables parameters to be chosen to improve shock capturing properties of numerical schemes. Moreover, **MIEELDLD** can also be used to gauge the shock capturing property of a numerical scheme better as compared to individual plots of AFM and RPE with respect to the phase angle since it is known that the inherent dissipation neutralises the inherent dispersion for a numerical scheme under consideration. We are currently using the technique to construct high order methods with low dispersion and low dissipation properties which approximate linear and non-linear equations in Computational Aeroacoustics.

12 Acknowledgements

This work was supported by a postdoctoral fellowship at the University of Cape Town, funded through the South African research Chair in Computational Mechanics. The author would like to thank the anonymous reviewers for their comments which were useful in clarifying and focusing the presentation.

References and Notes

Anderson DA, Tannehill JC, and Pletcher RH (1984). *Computational Fluid mechanics and Heat Transfer*. Hemisphere Publishing Corporation. 1984.

Appadu AR, Dauhoo MZ and Rughooputh SDDV (2008). Control of Numerical Effects of Dispersion and Dissipation in Numerical Schemes for Efficient Shock-Capturing Through an Optimal Courant Number. *Computers and Fluids 37*, (6), pp.767–783.

Appadu AR and Dauhoo MZ (2011). The Concept of Minimised Integrated Exponential Error for Low Dispersion and Low Dissipation. *International Journal for Numerical Methods in Fluids 65*, (5), pp. 578–601.

Appadu AR (In Press). Some Applications of the Concept of Minimized Integrated Exponential Error for Low Dispersion and Low Dissipation Schemes. *International Journal for Numerical Methods in Fluids*, DOI:10.1002/fld.2504.

Appadu AR (2012). Investigating the Shock-Capturing Properties of Some Composite Numerical Schemes for the 1-D Linear Advection Equation. *International Journal of Computer Applications in Technology 43*, (2).

Appadu AR and Dauhoo MZ. (2009). An Overview of Some High Order and Multi-Level Numerical Schemes in Computational Aeroacoustics. *Proceedings of the World Academy of Science, Engineering and Technology 38*, pp. 365–380.

Babarsky RJ and Sharpley RC (1997). Expanded Stability Through Higher Temporal Accuracy for Time-Centred Advection Schemes. *Monthly Weather Review 125*, pp. 1277–1295.

Boris JP and Book DL (1976). Flux-Corrected Transport, III: Minimal-Error FCT Algorithms. *Journal of Computational Physics 20*, pp. 397–431.

Carpenter K (1979). An Experimental Forecast using a Non-hydrostatic Mesoscale Model. *Quarterly Journal of Royal Meteorological Society 105*, pp. 629–655.

Courant R, Friedrichs, KO and Lewy H (1928). Oberdie partiellen differenzengleichurgen der Mathematischen Physik. *Mathematische Annalen 32*, pp. 32–74.

Crank J and Nicolson P (1947). A Practical Method for Numerical Evaluation of Solutions of Partial Differential Equations of the Heat Conduction. *Proceedings of the Cambridge Philosophical Society 43*, pp. 50–67.

Crowley (1968). Numerical Advection Experiments. *Monthly Weather Review 96*, pp. 1–11.

Cunge (1980). Practical Aspects of Computational River Hydraulics. *Monographs and Surveys in Water Resources Engineering.*

Dehghan M (2005). Quasi-implicit and two-level explicit finite-difference procedures for solving the one-dimensional advection equation. *Applied Mathematics and Computation 167*, pp. 46–67.

Fromm JE (1968). A Method for Reducing Dispersion in Convective Difference Schemes. *Journal of Computational Physics 3*, pp. 176–189.

Gadd (1978). A Numerical Scheme with Small Phase Speed Errors. *Quarterly Journal of the Royal Meteorological Society 104*, pp. 583–594.

Harten A, Engquist B, Osher S and Chkravarthy S (1987). 'Uniformly High-Order Accurate Nonoscillatory Schemes III'. *Journal of Computational Physics 71*, (2), pp. 231–303.

Hirsch C (1988). Numerical Computation of Internal and External Flows. *John Wiley and Sons*. 1988, 1.

Hirt CW (1968). Heuristic Stability theory for finite difference equations. *Journal of Computational Physics 2*, pp. 339–355.

Kreiss HO (1968). Stability theory for difference approximations of mixed initial boundary value problems. *Mathematics of Computation 104*, (22), pp. 703–714.

Lax PD and Wendroff B (1960). Systems of Conservation Laws. *Communications in Pure and Applied Mathematics 13*, pp. 217–237.

Leonard BP (1984). Third-Order Upwinding as a Rational Basis for Computational Fluid Dynamics. *Proceedings of Computational Techniques and Application*, CTAC-83, Elsevier/North-Holland, Amsterdam, 1984, p. 106–120. Eds J. Noye and C.A. Fletcher.

Laney CB (1998). Computational Gas Dynamics. *Cambridge University Press.*

Liu R (1995). The Remainder-Effect Analysis of Finite Difference Schmes and the Applications. *Applied Mathematics and Mechanics 16*, pp. 87–96.

Morton and Mayers (1994). Numerical Solution of Partial Differential Equations. Cambridge University Press.

Roberts and Weiss (1966). Convective Difference Schemes. *Mathematics of Computation 20*, pp. 272–299.

Rusanov (1970). On Difference Schemes of Third Order Accuracy for Nonlinear Hyperbolic Systems. *Journal of Computational Physics 5*, pp. 507–516.

Tam and Webb (1993). Dispersion-Relation-Preserving Finite Difference Schemes for Computational Aeroacoustics. *Journal of Computational Physics 107*, pp. 262–281.

Trac and Pen (2003). A Primer on Eulerian Computational Fluid Dynamics for Astrophysics. *Astronomical Society of the Pacific 115*, pp. 303–321.

Von Neumann and Richtmyer (1950). A Method for the Numerical Calculation of Hydrodynamic Shocks. *Journal of Applied Physics 21*, pp. 232–237.

Wang J (2010). Accurate and Efficient Difference Methods for Linear Advection-Diffusion Equations. *International Journal of Applied Mathematics and Mechanics 6*, (7), pp. 63–73.

Warming R.F. and Beam (1976). Upwind Second-Order Difference Schemes and Applications in Aerodynamic Flows. *AIAA Journal14*, pp. 1241–1249.

Warming and Hyett (1974). The Modified Equation Approach to the Stability and Accuracy of Finite Difference Method. *Journal of Computational Physics 14*, pp. 159–179.

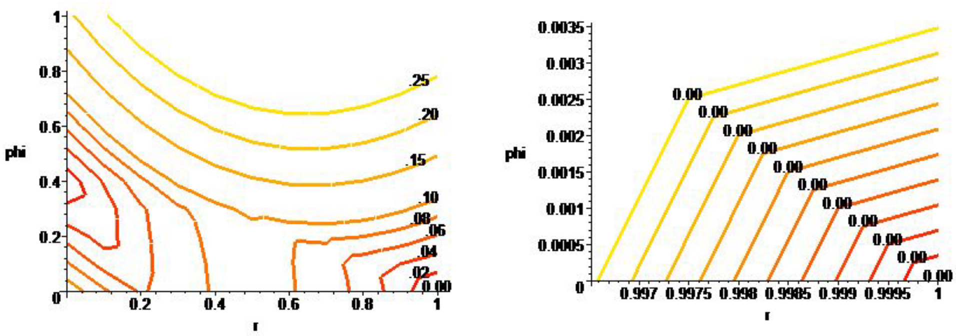

(a) Contour Plot

(b) Zoomed plot for least values of **IEELDLD**

Figure 1 Contour Plot of **IEELDLD** vs ϕ vs r for the case $\theta = 1$ and $\gamma_1 = 0$ for the numerical scheme described by Eq. (4).

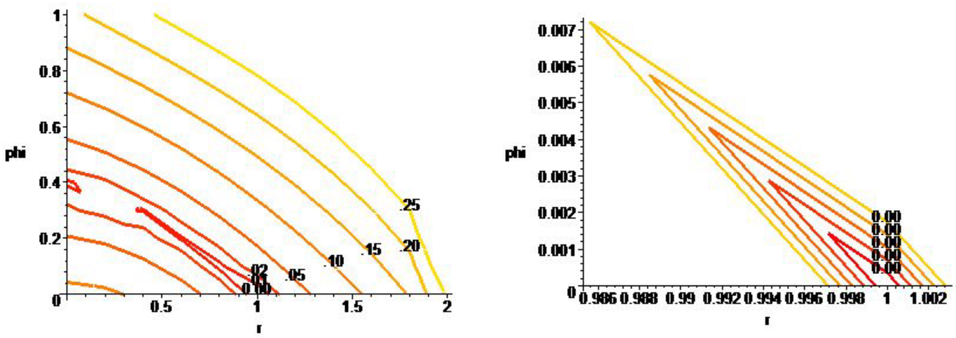

(a) Contour plot

(b) Zoomed plot with least values for **IEELDLD**

Figure 2 Contour Plot of **IEELDLD** vs ϕ vs r for the case $\theta = r$ and $\gamma_1 = 0$ for the numerical scheme described by Eq. (4).

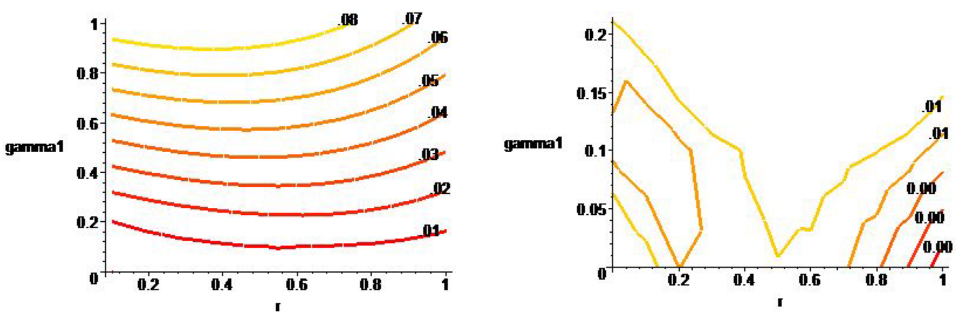

(a)

(b) Zoomed contour plot

Figure 3 Contour Plot of **IEELDLD** vs γ_1 vs r for the case $\theta = r$ and $\phi = \dfrac{1 - r^2}{3}$ for the numerical scheme described by Eq. (4).

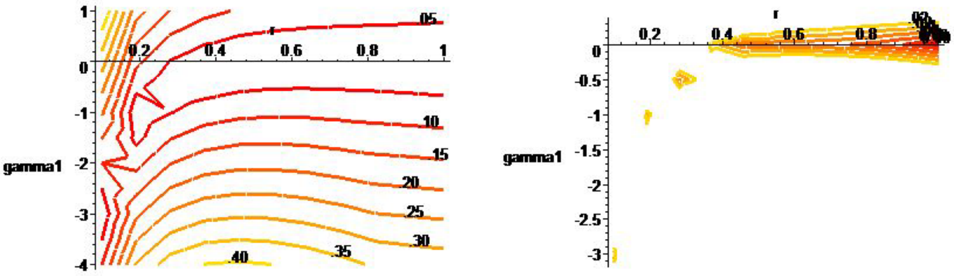

(a) Contour plot

(b) Zoomed plot with least values of **IEELDLD**

Figure 4 Contour plot of **IEELDLD** v/s γ_1 vs r for the case $\theta = r$ and $\phi = \dfrac{2(1-r^4)}{15r}$

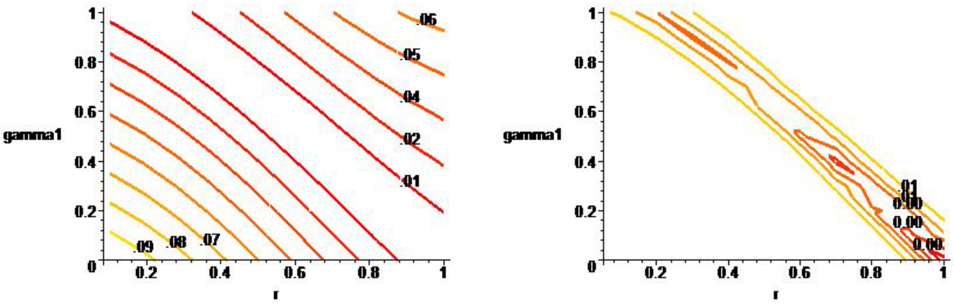

(a) Contour Plot

(b) Zoomed plot for least values of **IEELDLD**.

Figure 5 Contour Plot of **IEELDLD** v/s γ_1 vs r for the case $\theta = r$ and $\phi = \dfrac{r(1-r^2)}{6}$, for the numerical scheme described by Eq. (4).

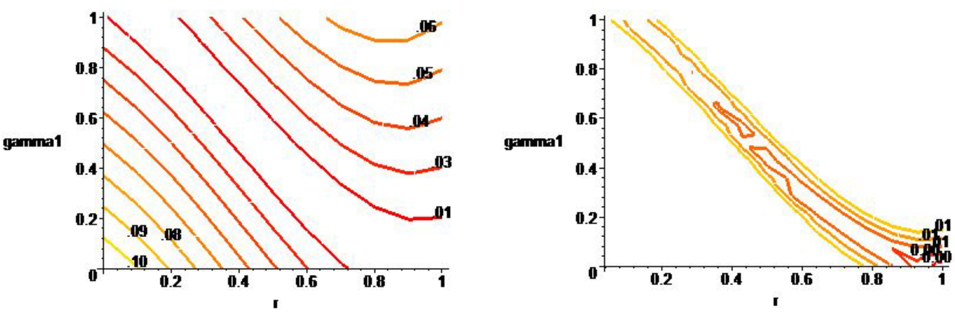

(a) Contour Plot

(b) Zoomed plot for least values of **IEELDLD**

Figure 6 Contour Plot of **IEELDLD** v/s γ_1 vs r for the case $\theta = r$ and $\phi = \dfrac{r(1-r^2)}{3}$, for the numerical scheme described by Eq. (4).

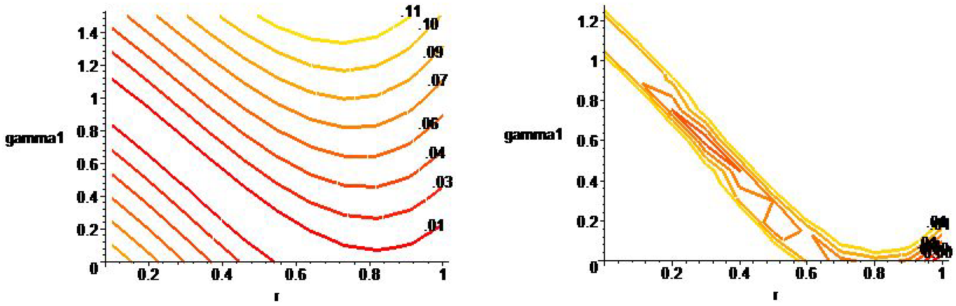

(a) Contour Plot

(b) Zoomed Plot for least values of **IEELDLD**

Figure 7 Contour Plot of **IEELDLD** vs γ_1 vs r for the case $\theta = r$ and $\phi = \dfrac{r\,(1-r^2)}{2}$, for the numerical scheme described by Eq. (4).

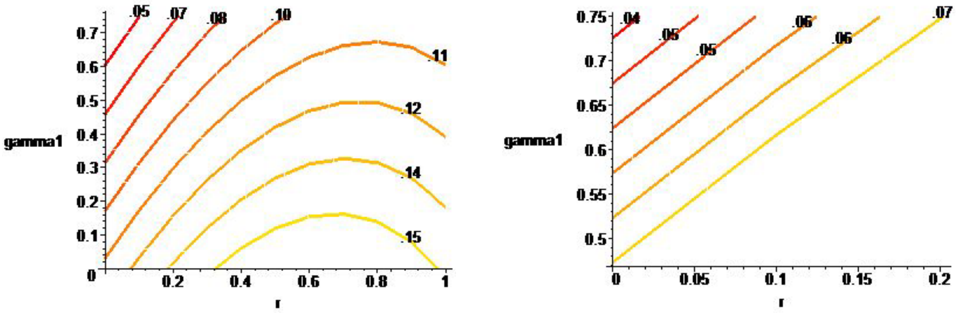

(a) Contour Plot

(b) Zoomed plot for least values of **IEELDLD**

Figure 8 Contour Plot of **IEELDLD** v/s γ_1 vs r for the case $\theta = r$ and $\phi = -\dfrac{r}{2}$

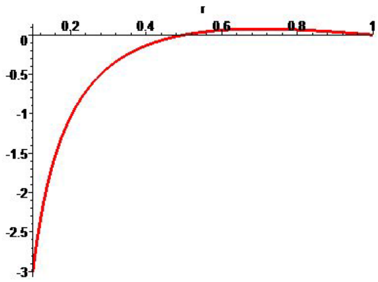

(a) Rusanov's third order scheme

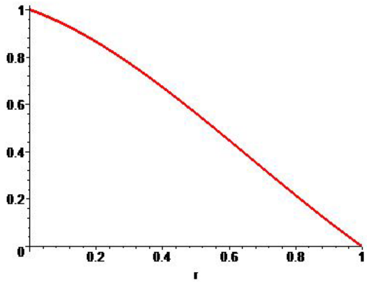

(b) Rusanov's fourth order scheme

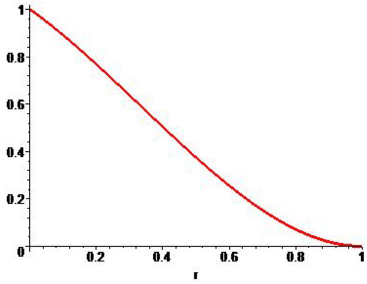

(c) Carpenter's scheme

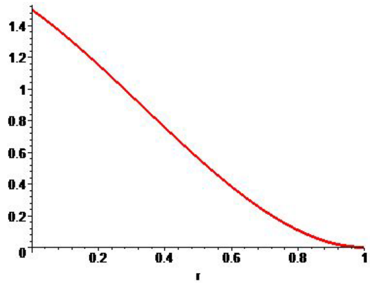

(d) Gadd's scheme

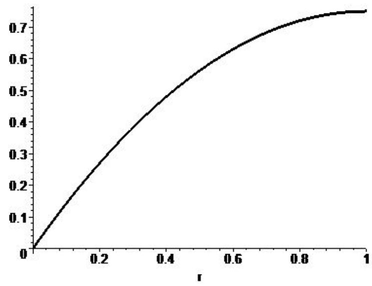

(e) Crowley scheme

Figure 9 Contour Plot of γ_1 vs r for some explicit methods with $\theta = r$

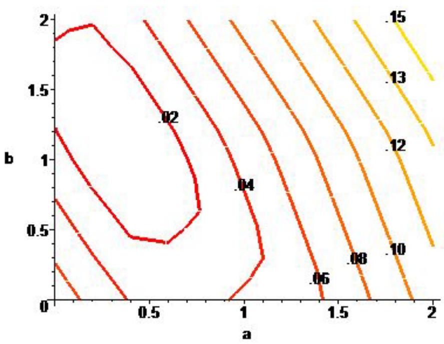

(a)

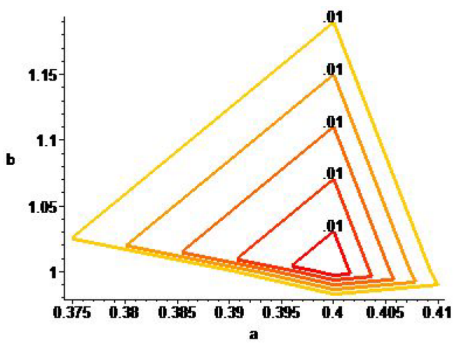

(b) zoomed plot for least values

Figure 10 Contour Plot of **IEELDLD** vs a vs b for the new optimised scheme obtained on modifying Carpenter's and Gadd numerical schemes.

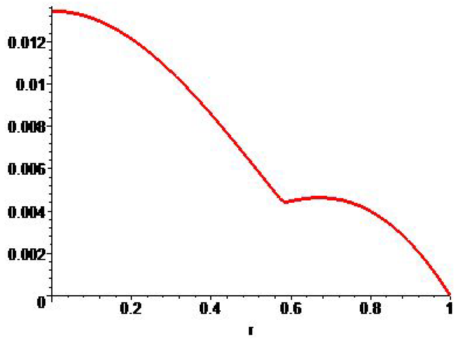

(a) Carpenter's scheme

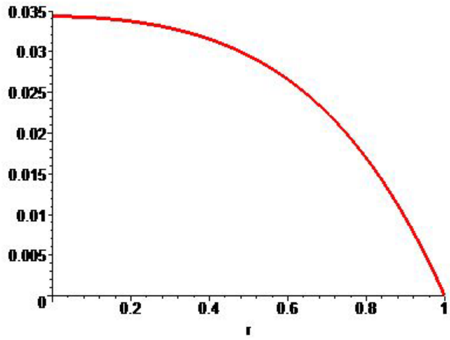

(b) Gadd's scheme

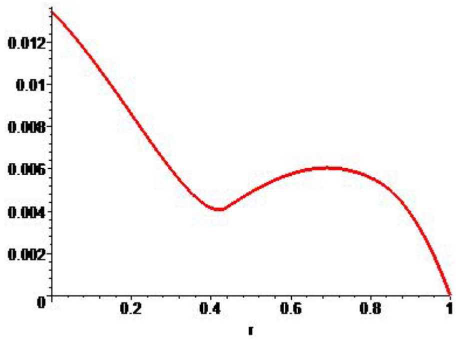

(c) Explicit AR scheme

Figure 11 Plot of **IEELDLD** vs r for the Carpenter, Gadd and the explicit AR schemes.

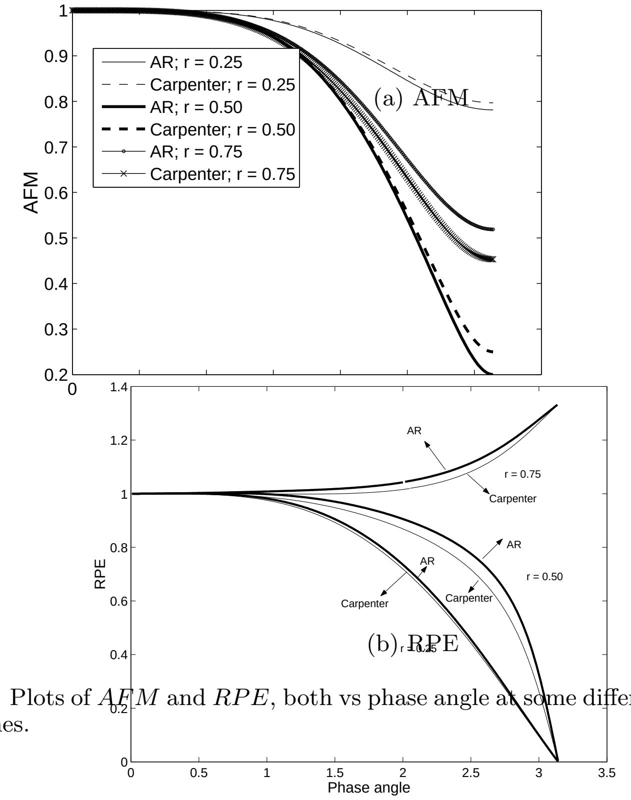

Figure 12 Plots of AFM and RPE, both vs phase angle at some different values of cfl for the Carpenter and AR schemes.

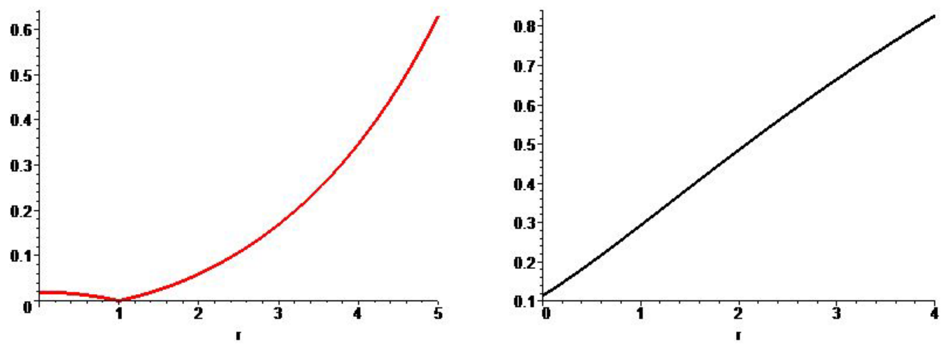

(a) Box scheme (b) Roberts and Weiss scheme

Figure 13 Plot of **IEELDLD** vs r for the Box scheme and Roberts and Weiss scheme.

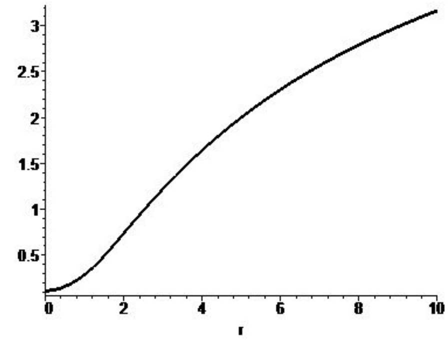

Figure 14 Plot of **IEELDLD** vs r for the Backward in Time and Centred in Space Scheme.

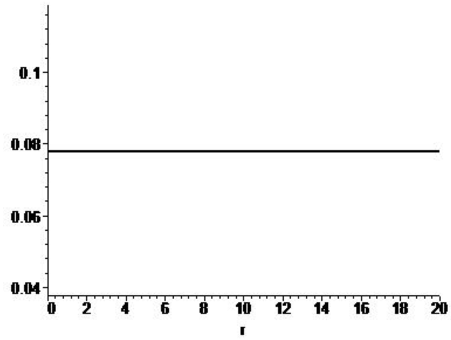

(b) **IEELDLD** vs r

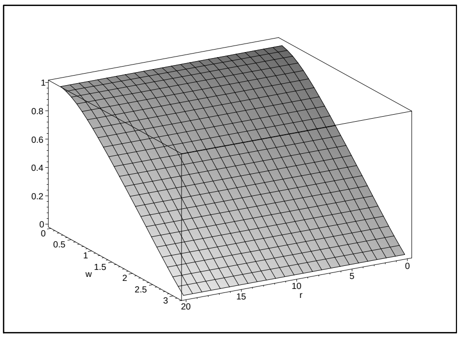

(a) RPE vs r vs w

Figure 15 Plots of the RPE and **IEELDLD** for the Crank Nicolson method.

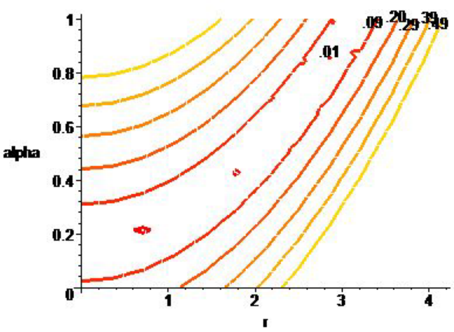

(a)

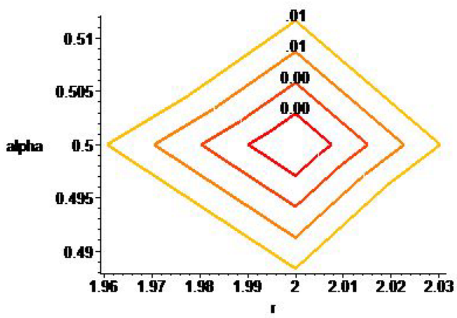

(b) Zoomed plot for smallest values of IEELDLD

Figure 16 Plot of **IEELDLD** vs α vs r for the α-optimised second order method.

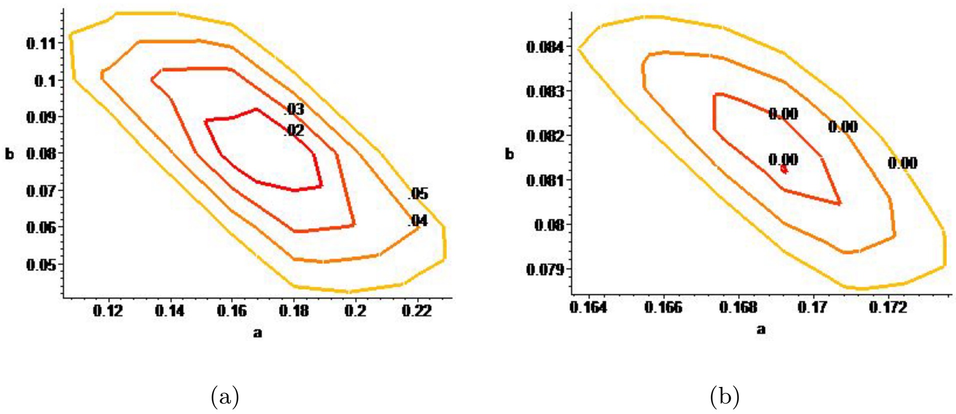

Figure 17 Contour plot of **IEELDLD** vs b vs a.

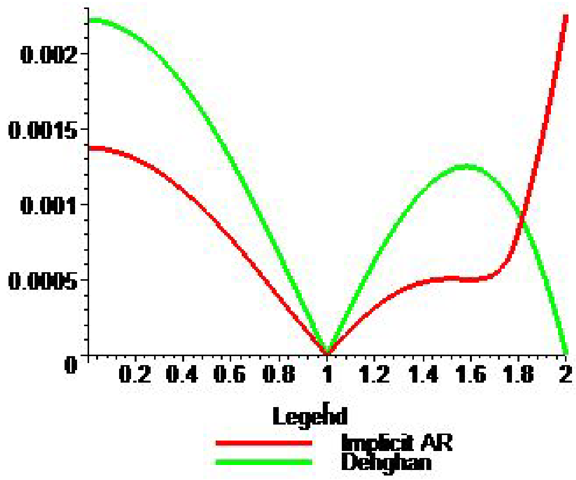

Figure 18 Plot of IEELDLD vs r for the second order implicit scheme derived by Dehghan (2005) and our new implicit scheme.